Cosmological Implications of the GWTC-3 Modified-Propagation Anomaly

Partial Hubble-Tension Relief and a CMB-Lensing Stress Test

Aiden B. Smith

February 10, 2026

Abstract

We propagate the posterior from the O3 dark-siren modified-gravity tension anomaly into late- and early-universe inference tests. The upstream anomaly analysis is archived on Zenodo (DOI: 10.5281/zenodo.18585598) with calibrated GR-injection baselines. In our constrained endpoint, anchor-based relief of the local-vs-Planck Hubble gap is moderate: $\mathcal{R}^{\rm GR}_{\rm anchor} = 0.246$ (p16/p50/p84 = 0.205/0.239/0.277), leaving a typical residual discrepancy of $\sim 1.17\sigma$.

The key result is a direct CAMB forecast against Planck 2018 lensing bandpowers using 64 posterior draws. The model predicts suppressed lensing power, with median shifts of -15.29% at $L \simeq 106$ and -9.49% at $L \simeq 286$ relative to the Planck-reference model. Draw-level fits are substantially worse than the Planck reference (median $\chi^2 = 51.77$ vs $\chi^2_{\rm ref} = 9.04$), and only 3.1% of draws outperform the reference; an independent 32-draw cross-check is more discrepant. Compressed $\theta_\star$ inversions under GR assumptions still bias inferred H_0 upward (mean $\Delta H_0 \simeq +1.14$ km s^{-1} Mpc^{-1} for fixed Ω_m, or $+4.57$ for lensing-proxy Ω_m).

Within this posterior projection, modified propagation shifts H_0 in the correct direction but is not sufficient to resolve the tension and is stressed by current CMB-lensing data unless additional perturbation-sector physics is introduced.

1 Motivation and Framing

This work treats the O3 signal phenomenologically: given the inferred modified-propagation posterior, what cosmological consequences follow? The O3 anomaly replication repository is public on Zenodo (DOI: 10.5281/zenodo.18585598) and defines the calibrated baseline used here. We do not re-argue the detection claim in this manuscript.

Modified GW propagation has been discussed in theory-forward frameworks [14, 15]. Here we instead use a data-driven posterior from the O3 anomaly and map it into: (i) late-time anchor relief, (ii) CMB-lensing compatibility, and (iii) GR mis-inference in compressed early-universe inversions.

2 Forecast Definitions

Posterior draws are taken from `outputs/finalization/highpower_multistart_v2/M0_start101` and propagated through synthetic anchor and CMB pipelines.

2.1 Late-time relief metrics

Define the baseline local-versus-Planck gap

$$\Delta H_0^{\rm base} \equiv \left| H_0^{\rm local} - H_0^{\rm Planck} \right|, \tag{1}$$

and the posterior-gap relief fraction

$$\mathcal{R}_{\text{post}} \equiv 1 - \frac{\left| H_{0,\text{MG}}^{\text{p50}} - H_0^{\text{local}} \right|}{\Delta H_0^{\text{base}}}. \tag{2}$$

The anchor-based estimator is

$$H_{0,\text{GR}}(z_a) = \frac{H_{\text{obs}}(z_a)}{\sqrt{\Omega_{m0}^{\text{GR}}(1+z_a)^3 + (1-\Omega_{m0}^{\text{GR}})}}, \tag{3}$$

$$\mathcal{R}_{\text{anchor}}^{\text{GR}} \equiv 1 - \frac{\left| \overline{H_{0,\text{GR}}} - H_0^{\text{local}} \right|}{\Delta H_0^{\text{base}}}. \tag{4}$$

2.2 CMB-facing tests

Two CMB-oriented tests are used:

1. draw-level propagation of $(H_0, \Omega_{m0}, \Omega_{k0}, \sigma_8)$ to Planck 2018 lensing bandpowers (direct CAMB mode),
2. compressed early-universe inversion using $\theta_\star = r_d/D_M(z_\star)$ under GR assumptions, with alternative assumptions for inferred Ω_m.

These are targeted forecasts, not full TT/TE/EE modified-gravity likelihood refits.

3 Results

3.1 Late-time relief remains partial

Using $z_a = \{0.2, 0.35, 0.5, 0.62\}$, 20,000 Monte Carlo replicates per anchor, and reference values $H_0^{\text{local}} = 73.0 \pm 1.0$ and $H_0^{\text{Planck}} = 67.4 \pm 0.5$:

- model-truth posterior gives $H_0^{\text{p50}} \simeq 70.39$ (p16/p84 = 67.70/73.39),
- constrained endpoint gives $\mathcal{R}_{\text{anchor}}^{\text{GR}}$ mean 0.246 with p16/p50/p84 = 0.205/0.239/0.277,
- typical residual local-versus-high-z discrepancy is $\sim 1.17\sigma$.

The joint transfer-bias fit over SN+BAO+CC (with O3 support as metadata) yields

$$\log \text{BF}_{\text{transfer/no-transfer}} = -0.533, \tag{5}$$

so explicit transfer terms are not preferred in this setup.

3.2 CMB lensing is the dominant stress test

For a direct CAMB run with 64 posterior draws against Planck 2018 lensing bandpowers:

$$\left.\frac{C_L^{\phi\phi}(\text{MG})}{C_L^{\phi\phi}(\text{Planck ref})}\right|_{L\approx 106} = 0.847^{+0.091}_{-0.127}, \quad \left.\frac{C_L^{\phi\phi}(\text{MG})}{C_L^{\phi\phi}(\text{Planck ref})}\right|_{L\approx 286} = 0.905^{+0.068}_{-0.080}, \tag{6}$$

corresponding to median suppressions of -15.29% and -9.49%.

Goodness-of-fit is strongly degraded relative to the Planck reference:

$$\chi^2_{\text{MG,draws}}\,(\text{median}) = 51.77, \qquad \chi^2_{\text{Planck ref}} = 9.04, \tag{7}$$

with only $p(\chi^2_{\text{draw}} < \chi^2_{\text{ref}}) = 3.1\%$. A cross-check run (32 draws from `M0_start303`) is more discrepant ($L \approx 106$: -18.66%, $L \approx 286$: -11.29%, $p_{\text{better}} = 0$).

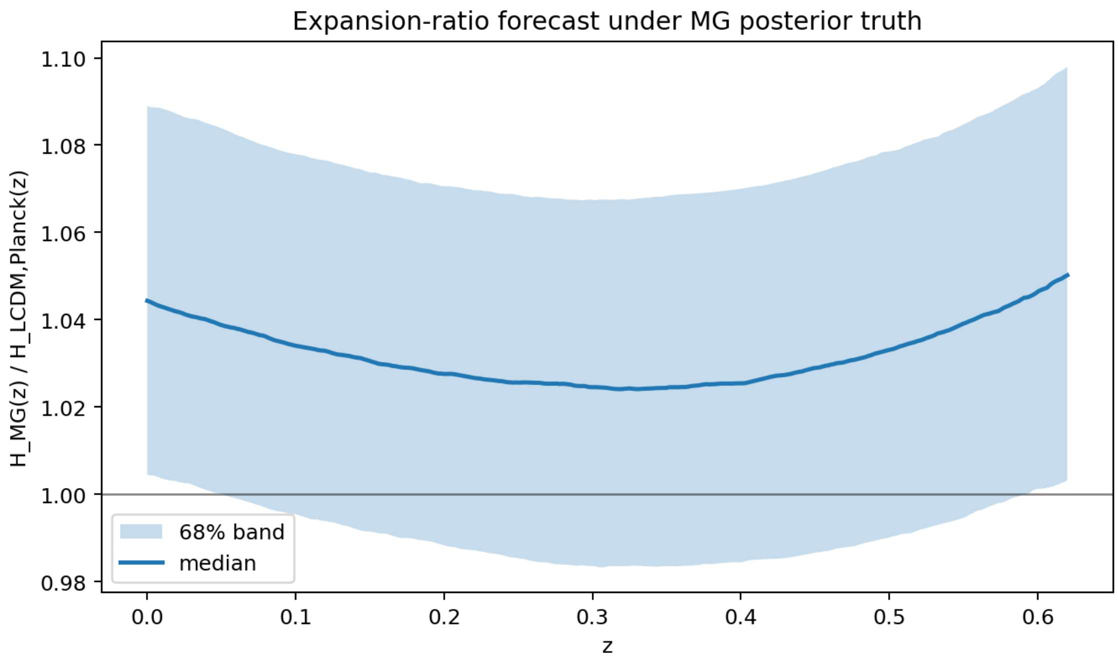

Figure 1: Forecasted expansion-ratio envelope under model truth: $H_{\mathrm{MG}}(z)/H_{\Lambda\mathrm{CDM,Planck}}(z)$.

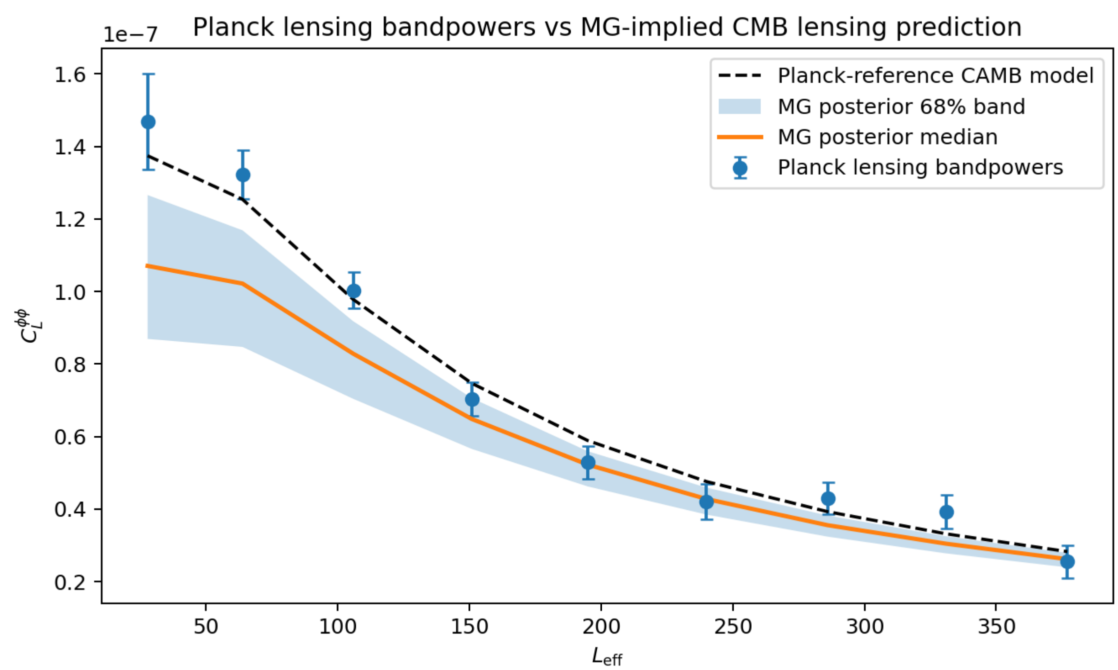

Figure 2: Planck 2018 lensing bandpowers (points) compared with the Planck-reference model (dashed) and MG posterior prediction band from the 64-draw CAMB forecast.

3.3 Early-universe GR mis-inference still biases H_0 upward

Compressed $\theta_\star$ inversion under GR assumptions gives systematic upward shifts in inferred H_0 relative to model-truth draws:

- fixed-Planck Ω_m: inferred H_0 mean 71.72, p50 72.55, mean $\Delta H_0 \simeq +1.14$ km s^{-1} Mpc^{-1},
- lensing-proxy Ω_m: inferred H_0 mean 75.15, p50 75.34, mean $\Delta H_0 \simeq +4.57$ km s^{-1} Mpc^{-1}.

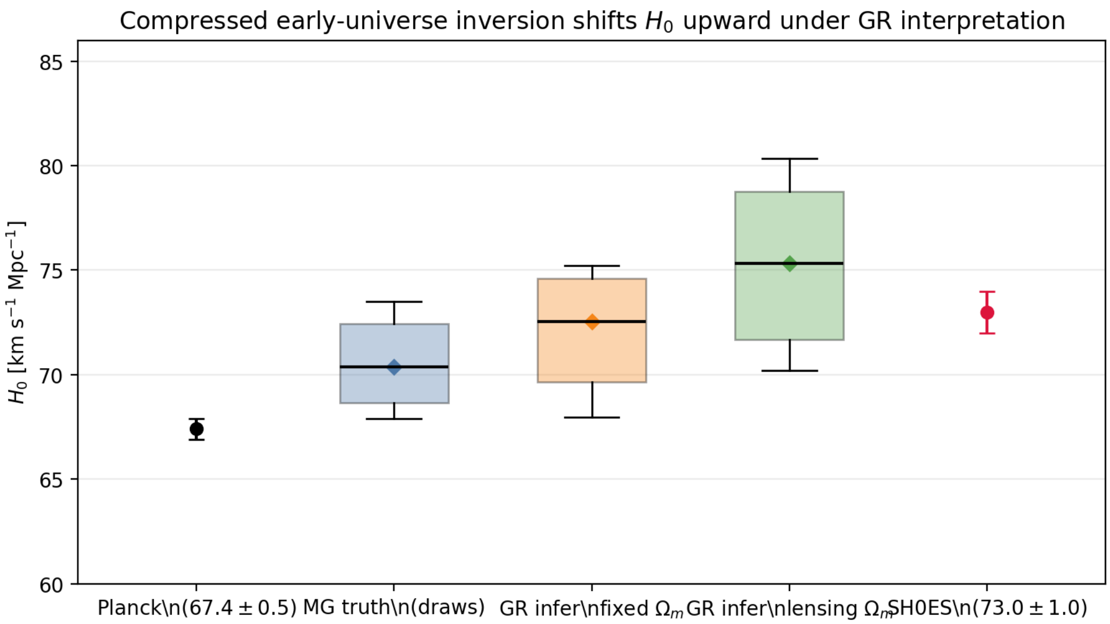

Figure 3: Comparative H_0 summary: Planck and SH0ES reference constraints (points with error bars), model-truth posterior, and GR-inferred compressed-CMB results under fixed-Ω_m and lensing-proxy-Ω_m assumptions (boxes with 16–84% whiskers).

4 Interpretation

The posterior-projection result is now clear: this mechanism moves inferred H_0 in the right direction but does not fully close the Hubble gap, and the same posterior predicts substantial CMB-lensing suppression that is disfavored by Planck lensing bandpowers in this implementation.

A pure amplitude rescue would require roughly $\sim 18\%$ extra lensing power near $L \sim 100$ (or $\sim 10\%$ near $L \sim 300$) relative to the current MG median prediction. That is outside the present draw-level amplitude proxy envelope ($A_{\mathrm{lens,proxy}}$ p84 ≈ 0.999). Therefore, evading the lensing stress test likely requires additional perturbation-sector physics (for example, nontrivial effective-Planck-mass evolution coupled to growth and Weyl potential transfer) beyond what is encoded in the current posterior projection.

Reproducibility

Core scripts used in this follow-up:

- `scripts/run_hubble_tension_mg_forecast.py`
- `scripts/run_hubble_tension_mg_forecast_robustness_grid.py`
- `scripts/run_hubble_tension_bias_transfer_sweep.py`
- `scripts/run_hubble_tension_final_relief_posterior.py`
- `scripts/run_joint_transfer_bias_fit.py`
- `scripts/run_hubble_tension_cmb_forecast.py`
- `scripts/run_hubble_tension_early_universe_bias.py`

Acknowledgments

This work relied extensively on A.I.-assisted tools for code development, pipeline execution support, figure generation, and manuscript drafting/editing.

Data Availability and DOIs

The follow-up uses posterior products from the O3 anomaly pipeline and public cosmology datasets. Data provenance and DOIs are:

- O3 modified-gravity tension anomaly repository (Zenodo): DOI 10.5281/zenodo.18585598.
- O3 search-sensitivity injection data used in upstream calibration (Zenodo): DOI 10.5281/zenodo.7890437.
- GWTC-3 catalog paper: DOI 10.1103/PhysRevX.13.041039.
- Pantheon+ cosmology constraints: DOI 10.3847/1538-4357/ac8e04.
- SH0ES local-H_0 reference: DOI 10.3847/2041-8213/ac5c5b.
- SDSS DR12 BOSS consensus BAO (source of `sdss_DR12Consensus_bao.dat`): DOI 10.1093/mnras/stx721.
- eBOSS DR16 cosmological compilation (source class for `sdss_DR16_LRG_BAO_DMDH.dat`): DOI 10.1103/PhysRevD.103.083533.
- DESI 2024 BAO cosmological constraints (source class for `desi_2024_gaussian_bao_ALL_GCcomb_mean.txt`): DOI 10.1088/1475-7516/2025/02/021.
- Cosmic-chronometer compilation components used in `Hz_BC03_all.dat`: DOIs 10.1088/1475-7516/2012/08/006, 10.1103/PhysRevD.71.123001, and 10.1088/1475-7516/2010/02/008.
- Planck 2018 cosmological parameters and lensing references: DOIs 10.1051/0004-6361/201833910 and 10.1051/0004-6361/201833886.

References

[1] A. B. Smith, "O3 Modified Gravity Tension Replication," Zenodo (2026), DOI: 10.5281/zenodo.18585598.

[2] LIGO Scientific Collaboration, Virgo Collaboration, and KAGRA Collaboration, "GWTC-3: Compact Binary Coalescences Observed by LIGO and Virgo During the Second Part of the Third Observing Run — O3 search sensitivity estimates," Zenodo (2023), DOI: 10.5281/zenodo.7890437.

[3] R. Abbott *et al.* (LIGO Scientific Collaboration, Virgo Collaboration, and KAGRA Collaboration), "GWTC-3: Compact Binary Coalescences Observed by LIGO and Virgo During the Second Part of the Third Observing Run," *Phys. Rev. X* **13**, 041039 (2023), DOI: 10.1103/PhysRevX.13.041039.

[4] D. Brout *et al.*, "The Pantheon+ Analysis: Cosmological Constraints," *Astrophys. J.* **938**, 110 (2022), DOI: 10.3847/1538-4357/ac8e04.

[5] A. G. Riess *et al.*, "A Comprehensive Measurement of the Local Value of the Hubble Constant with 1 km s^{-1} Mpc^{-1} Uncertainty from the Hubble Space Telescope and the SH0ES Team," *Astrophys. J. Lett.* **934**, L7 (2022), DOI: 10.3847/2041-8213/ac5c5b.

[6] S. Alam *et al.*, "The clustering of galaxies in the completed SDSS-III Baryon Oscillation Spectroscopic Survey: cosmological analysis of the DR12 galaxy sample," *Mon. Not. R. Astron. Soc.* **470**, 2617 (2017), DOI: 10.1093/mnras/stx721.

[7] S. Alam *et al.*, "Completed SDSS-IV extended Baryon Oscillation Spectroscopic Survey: Cosmological implications from two decades of spectroscopic surveys at the Apache Point Observatory," *Phys. Rev. D* **103**, 083533 (2021), DOI: 10.1103/PhysRevD.103.083533.

[8] DESI Collaboration, "DESI 2024 VI: cosmological constraints from the measurements of baryon acoustic oscillations," *J. Cosmol. Astropart. Phys.* **02** (2025) 021, DOI: 10.1088/1475-7516/2025/02/021.

[9] M. Moresco *et al.*, "Improved constraints on the expansion rate of the Universe up to $z \sim 1.1$ from the spectroscopic evolution of cosmic chronometers," *J. Cosmol. Astropart. Phys.* **08** (2012) 006, DOI: 10.1088/1475-7516/2012/08/006.

[10] J. Simon, L. Verde, and R. Jimenez, "Constraints on the redshift dependence of the dark energy potential," *Phys. Rev. D* **71**, 123001 (2005), DOI: 10.1103/PhysRevD.71.123001.

[11] D. Stern *et al.*, "Cosmic chronometers: constraining the equation of state of dark energy. I: $H(z)$ measurements," *J. Cosmol. Astropart. Phys.* **02** (2010) 008, DOI: 10.1088/1475-7516/2010/02/008.

[12] N. Aghanim *et al.* (Planck Collaboration), "Planck 2018 results. VI. Cosmological parameters," *Astron. Astrophys.* **641**, A6 (2020), DOI: 10.1051/0004-6361/201833910.

[13] N. Aghanim *et al.* (Planck Collaboration), "Planck 2018 results. VIII. Gravitational lensing," *Astron. Astrophys.* **641**, A8 (2020), DOI: 10.1051/0004-6361/201833886.

[14] E. Belgacem, Y. Dirian, S. Foffa, and M. Maggiore, "Modified gravitational-wave propagation and standard sirens," *Phys. Rev. D* **98**, 023510 (2018), DOI: 10.1103/PhysRevD.98.023510.

[15] A. Nishizawa, "Generalized framework for testing gravity with gravitational-wave propagation," *Phys. Rev. D* **97**, 104037 (2018), DOI: 10.1103/PhysRevD.97.104037.